Multi-vehicle Cooperative Control for Load Transportation

Tiago Valentim
tiago.valentim@tecnico.ulisboa.pt

Instituto Superior Técnico, Universidade de Lisboa, Portugal

June 2019

Abstract

This work proposes a cooperative control solution to the problem of transporting a suspended load using multiple quadrotor vehicles. The problem is addressed for two quadrotors, with a methodology that can be generalized for any number of quadrotors. A dynamic model of the system is developed, considering a point-mass load, rigid massless cables, and neglecting aerodynamic effects of the cables. The concept of differential flatness is explored and a new set of flat outputs, which can be used to fully characterize the state of the system, is proposed. A nonlinear Lyapunov-based controller in cascaded form is derived, by defining adequate mappings between the cable tension vectors and the quadrotor thrust vectors and exploring the analogy with the problem of controlling a single quadrotor. Simulation results are presented for tracking of load trajectories. Comparisons are made with a free-flying quadrotor control scheme to highlight the enhanced performance of the proposed scheme. Future work is then suggested to increase the accuracy of the full model, generalizing the control scheme and referring to a few estimation problems.

Keywords: nonlinear control, differential flatness, cascaded systems, autonomous vehicles, slung-load transportation

1. Introduction

In recent years, there has been a growing use of Unmanned Aerial Vehicles (UAVs) for various applications. In particular, quadrotor UAVs have received a lot of attention due to their high maneuverability in 3D environments, high thrust to weight ratio and reduced mechanical complexity. Applications include coverage of media events (photography and filming), infrastructure inspections, and mobile sensor networks, to name a few. Among these applications, load transportation is a topic that has been explored for several years. As highlighted in [17], it has gained importance in both civil and military applications, taking advantage of the vehicles' ability to describe precise trajectories for transportation of fragile cargo.

Different solutions have been considered when using a quadrotor for load transportation. The use of grips to attach the load to the quadrotor has been previously studied. Although this approach simplifies the underlying model, it also reduces the maneuverability of the quadrotor due to the added inertia and does not provide a safety distance between the load and the vehicle, which may be required when attaching and detaching the load. Cable-slung transportation has also been studied. It maintains the maneuverability of the quadrotor by separating the load inertia but increases the complexity of the underlying model due to the interactions through the cable, restricting the vehicle's DOFs (degrees of freedom). A viable solution to carry heavier loads is to use multiple vehicles instead of increasing the size and consequently the maximum thrust of the vehicle. By developing proper controllers for these systems, a new transport service can be provided for a multitude of trajectories without compromising the load.

Research on slung-load transportation goes from path-planning to control system design and estimation problems. Several results available in the literature use the concept of differential flatness, which defines a class of dynamical systems for which all states and inputs can be described as functions of the so-called flat output and its time derivatives. This property has been explored to address both motion planning and tracking control problems. For example, the work reported in [10] relies on the fact that a free-flying quadrotor is differentially flat to define reference trajectories that minimize the sixth order time derivative of the quadrotors's position to design smooth trajectories, developing afterwards a nonlinear controller for trajectory tracking. The work in [16] shows that a system comprised of a single quadrotor and a load connected by a inelastic massless cable is differentially flat and extends also the definition for the full hybrid system that results from considering the case when the cable is not taut. This concept is further developed in [15], con-

sidering a rigid body load and proving differential flatness for 3 or more quadrotors. The work in [4] proves differential flatness for a system comprised of a point-mass load attached to a single quadrotor, modeling the cable as a series of links with the mass concentrated at the end point. It then constructs a LQR (Linear Quadratic Regulator) controller for the case of one quadrotor, by linearizing the dynamics directly in the manifold. The work in [8] applies geometric control to address the problem of slung-load transportation using an arbitrary number of quadrotors and a point-mass load, considering both relative and inertial vehicle formation control modes. A proof of convergence is provided, using an inner-outer loop control structure and arguments from singular perturbation theory. In [7] this control method is extended to consider a rigid-body load. [12] analyse the full model of a single quadrotor and a load and define the domains for the inputs and angular velocity of the cable where the cables remain taut and the quadrotor's thrust points outwards to avoid compression forces on the cables. Two alternative controllers providing exponential convergence are then proposed. In [11] the problem of controlling two drones with a slung-load is addressed by separating the problem into three decoupled systems and controlling each one separately: one for position, another for the yaw angles and a final one for the plane defined by the two cables. The work in [3] develops further from [15] by describing the cable via a mass-spring model to account for its elasticity. Although the resulting system is not differentially flat, a geometric controller is proposed and convergence is proven for the reduced dynamics via single perturbation theory.

In this work, we propose a cooperative control scheme for multi-vehicle load transportation, exploring the definition of a new set of flat outputs. These include the position of the load and a set of angles that completely define the cable directions and consequently the relative positions of the quadrotors. Explicit mappings between the cable tension vectors and the quadrotor thrust vectors are then explored to define an error system, starting with the load position error, progressing to the cable direction errors, and ending with quadrotors' thrust direction error. The resulting closed-loop system takes the form of a cascaded system, whose origin is shown to be asymptotically stable.

This thesis can be divided in several chapters. In chapter 2, theoretical background is given by analysing more basic control problems for quadrotor UAVs: first considering the free-flying quadrotor then the control problem for a single quadrotor with a slung-load, establishing parallels between these problems and the main implementation. In chapter 3, the concept of differential flatness is explained, and a novel set of flat outputs is defined and applied to the problem of two quadrotors transporting a load, followed by the description of the control design. In chapter 4, simulation results for multiple trajectories are presented and discussed, with added testing for different configurations of the system. In chapter 5, some final remarks are made, outlining paths for future development on this subject based on the proposed work.

2. Background

The theoretical background for this proposed work is composed of developing two control systems for a free-flying quadrotor and for the case of one quadrotor transporting a slung-load. Main theorems used for nonlinear control systems are referenced from [14] and [2]. The full analysis of this model and deductions can be consulted in the full proposed work.

3. Design of the tracking controller for load transportation

The following section will state the control problem, develop the full load model, discuss differential flatness, present a novel set of flat outputs and develop the nonlinear controller, with and without an inner loop obtained by a backstepping process [2].

3.1. Problem Statement

Consider two quadrotors, with masses m_{Q_1} and m_{Q_2}, connected by massless, rigid links with lengths l_1 and l_2 to a point-mass load with mass m_l. An inertial reference frame $\{I\}$ is introduced, along with two body reference frames $\{B_i\}$ where $i \in \{1, 2\}$, each one fixed to the center of mass of quadrotor i. The inertial reference frame has its z axis pointing downwards, in the direction of the gravity vector, which is assumed to be constant. As shown in Fig. 1, let the direction of each cable i be described by a unit vector $\boldsymbol{q}_i \in \mathbb{S}^2$, where $\mathbb{S}^2 = \{\boldsymbol{q}_i \in \mathbb{R}^3 \mid \|\boldsymbol{q}_i\| = 1\}$, expressed in the inertial reference frame and centered at the origin of the body frame $\{B_i\}$. The load position expressed in $\{I\}$ is defined as $\boldsymbol{x}_l$ and the orientation of quadrotor i, or more specifically, the rotation matrix from $\{B_i\}$ to $\{I\}$ is defined as $R_{Q_i} \in \mathbb{SO}(3)$, where $\mathbb{SO}(3) = \{RR^T = I \mid det(R) = 1\}$ denotes the Special Orthogonal Group of order 3.

Within this setting, the control objective consists of designing a control law to achieve tracking of a desired trajectory for the load, i.e. guarantee that the load position $\boldsymbol{x}_l(t)$ converges asymtptotically to the desired position $\boldsymbol{x}_{l_d}(t)$.

Given the rigid link assumption, it immediately follows that

$$\boldsymbol{x}_{Q_i} = \boldsymbol{x}_l - l_i \boldsymbol{q}_i \quad , \tag{1}$$

where $\boldsymbol{x}_{Q_i}$ is the position of quadrotor i expressed in $\{I\}$ (see Fig. 1). By Newton's Law, the following

expression can be obtained for the total accelerations of the load and quadrotors

$$\begin{cases} m_l \ddot{\boldsymbol{x}}_l = -T_1 \boldsymbol{q}_1 - T_2 \boldsymbol{q}_2 + m_l g \boldsymbol{e}_3 = -T_{L_t} \boldsymbol{q}_t + m_l g \boldsymbol{e}_3 \\ m_{Q_i} \ddot{\boldsymbol{x}}_{Q_i} = T_i \boldsymbol{q}_i - T_{Q_i} \boldsymbol{r}_{Q_i} + m_{Q_i} g \boldsymbol{e}_3 \end{cases} \tag{2}$$

where $\ddot{\boldsymbol{x}}_l$ denotes the load linear acceleration, $\ddot{\boldsymbol{x}}_{Q_i}$ the acceleration of quadrotor i, g the gravitational acceleration, T_i the tension applied by link i, T_{Q_i} the thrust applied by quadrotor i, and $\boldsymbol{r}_{Q_i}$ the direction of that thrust, which coincides with the z-axis of the vehicle. The scalar T_{L_t} and unit vector $\boldsymbol{q}_t \in \mathbb{S}^2$ define the total tension norm and direction, respectively, and are such that $T_t \boldsymbol{q}_t = T_1 \boldsymbol{q}_1 + T_2 \boldsymbol{q}_2$.

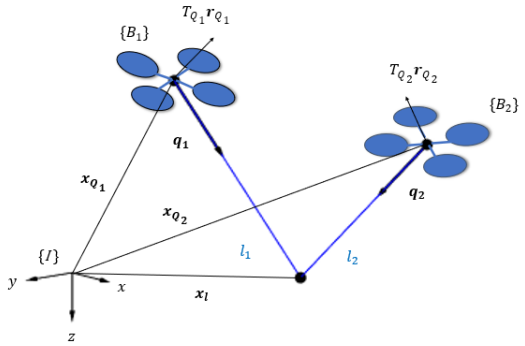

Figure 1: Illustration of the problem statement (n = 2)

For the sake of simplicity, we assume that, for each quadrotor, an inner loop controller provides tracking of angular velocity commands and consider only the kinematics of $\boldsymbol{r}_{Q_i}$, assuming that the extra angular degree of freedom is independently controlled.

Using (1) and (2) similarly to [8], and performing additional algebraic manipulations, the complete model can be written as

$$\begin{cases} \dot{\boldsymbol{x}}_l = \boldsymbol{v}_l \\ \dot{\boldsymbol{v}}_l = g \boldsymbol{e}_3 - M_q^{-1} \sum_{i=1}^{n} \alpha_i \boldsymbol{q}_i \\ \ddot{\boldsymbol{q}}_i = -\|\dot{\boldsymbol{q}}_i\|^2 \boldsymbol{q}_i \\ \qquad + \frac{1}{l_i} \Pi_{q_i} \left(\frac{1}{m_{Q_i}} T_{Q_i} \boldsymbol{r}_{Q_i} - M_q^{-1} \sum_{j=1}^{n} \alpha_j \boldsymbol{q}_j \right) \\ \dot{\boldsymbol{r}}_{Q_i} = \boldsymbol{u}_{Q_i} \end{cases} \tag{3}$$

where the following variables are introduced

- $\boldsymbol{v}_l$ is the velocity of the load;
- M_q is the positive definite symmetric matrix given by $M_q = m_l I + \sum_{i=1}^{n} m_{Q_i} \boldsymbol{q}_i \boldsymbol{q}_i^T$
- α_i is an auxiliary variable given by $\alpha_i = \boldsymbol{q}_i^T T_{Q_i} \boldsymbol{r}_{Q_i} + m_{Q_i} l_i \|\dot{\boldsymbol{q}}_i\|^2$
- $\Pi_{q_i} \boldsymbol{y}$ represents the perpendicular component of vector y with respect to $\boldsymbol{q}_i$
- $\boldsymbol{u}_{Q_i}$ is the simplified quadrotor angular velocity input, which satisfies $\boldsymbol{r}_{Q_i}^T \boldsymbol{u}_{Q_i} = 0$.

One aspect to consider when analysing the model equations is the fact for each quadrotor only the thrust component that is parallel to the respective links $\boldsymbol{q}_i^T T_{Q_i} \boldsymbol{r}_{Q_i}$ has an effect on the dynamics of the load, whereas the perpendicular component of the thrust $\Pi_{\boldsymbol{q}_i} T_{Q_i} \boldsymbol{r}_{Q_i}$ can be used to control the direction of cable i. This already gives insight to the control strategy that will be developed in the following sections.

3.2. Differential flatness of the system - describing the flat outputs

Differential flatness is a property of some systems and can be considered as a generalization of linear systems. These systems benefit from certain properties and characteristics that help to construct smooth trajectories for a system by using certain variables and to develop control methods for nonlinear systems with advantageous properties. In a more formal manner, if we consider a system with states $\boldsymbol{x} \in \mathbb{R}^n$ and inputs $\boldsymbol{u} \in \mathbb{R}^p$, a system is differentially flat if there exist a set of outputs $\boldsymbol{y} = h(\boldsymbol{x}, \boldsymbol{u}, \dot{\boldsymbol{u}}, \ddot{\boldsymbol{u}}, ..., \boldsymbol{u}^{(p)}) \in \mathbb{R}^p$, called the flat outputs, such that

$$\begin{cases} x = h(\boldsymbol{y}, \dot{\boldsymbol{y}}, \ddot{\boldsymbol{y}}, ..., \boldsymbol{y}^{(p)}) \\ u = f(\boldsymbol{y}, \dot{\boldsymbol{y}}, \ddot{\boldsymbol{y}}, ..., \boldsymbol{y}^{(p)}). \end{cases}$$

[9] highlights an important property of differentially flat systems, which states that the problem of controlling a differentially flat system becomes equivalent to controlling a trivial system composed of only integrators, by using a suitable coordinate change and dynamic feedback or finding an equivalent flat system. As long as the coordinate change is well defined in a certain region, an injective mapping and equivalence between the original system and the trivial system can be established. As pointed out in the introduction, other authors have tackled the load transportation problem by defining a set of flat outputs for the system. For the particular case of a point-mass model and n quadrotors, the system is differentially flat, with flat outputs given by the yaw angles of the quadrotors ψ_i, the position of the load $\boldsymbol{x}_l$ and the values of $n-1$ tension vectors $T_i \boldsymbol{q}_i$. In this section an alternative set of flat outputs is proposed, from which the flat outputs described previously can be reached. The problem is defined for the case of a point mass load and two quadrotors.

Figure 2 displays the problem configuration, introducing the angles β_1, β_2, and γ, which define the

orientation of $\boldsymbol{q}_1$ and $\boldsymbol{q}_2$ relative $\boldsymbol{q}_t$ and satisfy

$$\begin{cases} \beta_1 = arcos(\boldsymbol{q}_t \cdot \boldsymbol{q}_1), & \beta_1 \in [0, \pi] \\ \beta_2 = arcos(\boldsymbol{q}_t \cdot \boldsymbol{q}_2), & \beta_2 \in [0, \pi] \\ \gamma = asin(-\frac{\boldsymbol{q}_2 \times \boldsymbol{q}_1}{\|\boldsymbol{q}_2 \times \boldsymbol{q}_1\|} \cdot \boldsymbol{e}'_y), & \gamma \in [0, 2\pi[, \end{cases}$$

where $\boldsymbol{q}_t$ is total tension direction introduced in (2). Given $\boldsymbol{q}_t$, β_1, β_2, and γ, the tension directions $\boldsymbol{q}_1$ and $\boldsymbol{q}_2$ can be specified as

$$\boldsymbol{q}_i = R_{aux} R_x(\gamma) R_z((-1)^{i-1}\beta_i)\boldsymbol{e}_1, \tag{4}$$

where

$$R_{aux} = R_y(\phi_t) R_z(\theta_t)$$

and

$$\begin{cases} \phi_t = arcos(\frac{T_t \cdot \boldsymbol{e}_x}{\|T_{L_{zx}}\|}), & 0 < \phi_t \leq \pi \\ \phi_t = 2\pi - arcos(\frac{T_t \cdot \boldsymbol{e}_x}{\|T_{L_{zx}}\|}), & \pi < \phi_t \leq 2\pi, \\ \quad with \quad T_{L_{zx}} = [T_{L_t} \cdot \boldsymbol{e}_1 \; 0 \; T_{L_t} \cdot \boldsymbol{e}_3]\boldsymbol{q}_t \end{cases}$$

and $\theta_t = \frac{\pi}{2} - arcos(\frac{T_t \cdot \boldsymbol{e}_y}{\|T_{L_t}\boldsymbol{q}_t\|}) \in [0, \pi]$, representing the azimute and elevation angles of the total tension vector with respect to the inertial reference frame. The rotation matrix R_{aux} defines the orientation of an auxiliary reference frame with x-axis aligned with $\boldsymbol{q}_t$ relative to the inertial frame.

Assumption 1. $T_{L_t}\boldsymbol{q}_t$ is always non-zero and the third component is always non-zero, with each cable always being taut, i.e, $T_{Li} \neq 0$.

This assumption guarantees that the plane formed by $\boldsymbol{q}_1$ and $\boldsymbol{q}_2$ (which also contains $\boldsymbol{q}_t$) is always well-defined and a mapping for the thrust values of each quadrotor is guaranteed to exist.

Theorem 2. *Under assumption 1, the system presented in* (3) *is differentially flat, with the set of flat outputs given by* $\boldsymbol{x}_l$, ψ_1, ψ_2, β_1, β_2 *and* γ.

Proof. By use of (2), given a desired trajectory for the load $\boldsymbol{x}_l$ and respective acceleration $\ddot{\boldsymbol{x}}_l$, we can calculate a desired Tension vector $T_{L_t}\boldsymbol{q}_t$.

Given β_1, β_2, and γ, the directions $\boldsymbol{q}_1$ and $\boldsymbol{q}_2$ can be immediately recovered from (4). To recover T_1 and T_2 we note that $T_1\boldsymbol{q}_1 + T_2\boldsymbol{q}_2 = T_{L_t}\boldsymbol{q}_t$. It follows that

$$R_{aux} R_x(\gamma)(T_1 R_y(\beta_1) + T_2 R_y(-\beta_2))\boldsymbol{e}_1 = T_t \boldsymbol{q}_t,$$

yielding

$$\begin{bmatrix} cos(\beta_1) & cos(\beta_2) \\ sin(\beta_1) & -sin(\beta_2) \end{bmatrix} \begin{bmatrix} T_{L_1} \\ T_{L_2} \end{bmatrix} = \begin{bmatrix} T_{L_t} \\ 0 \end{bmatrix} \tag{5}$$

Thus, from $\ddot{\boldsymbol{x}}_l$, β_1, β_2, and γ the tension of either one of the cables can be determined, which together with the yaw angles of the quadrotors ψ_1 and ψ_2 form the outputs that are shown to be flat in [15]. □

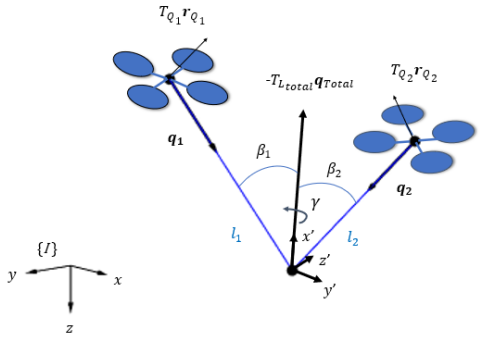

Figure 2: Flat outputs Illustration (n = 2)

Notice that the transformation is only well defined if the matrix in (5) is invertible, which is the case if β_1 and $\beta_2 \in]0, \frac{\pi}{2}[$ rad. One can consider broader cases where one of the cables is pointing towards the opposite direction of the required total tension, however, for practical cases and when considering the total amount of thrust required for such configurations, these are not attractive. Given the identified set of flat outputs, path planning can be performed to generate reference trajectories, which can then be used for control system design.

3.3. Outer loop control scheme

In this section, the control formulation will be given for the configuration presented in 3.1. An analogy to a free flying quadrotor control formulation will be made, following an approach similar to the one in [1] for the case of a single quadrotor with suspended load, but now extended to the case of two vehicles. To simplify the controller design and follow a constructive approach, a simplified model that neglects the orientation dynamics of both quadrotors is chosen as a starting point, meaning that $T_{Q_i}\boldsymbol{r}_{Q_i}$ can be set instantaneously and used as inputs. Under this assumption, a parallel with the dynamics for a free flying quadrotor can be drawn by applying an adequate change of variables.

Considering the definition of the total tension vector given in (2) and new variables τ_1 and τ_2 that satisfy $\boldsymbol{\tau}_i = \frac{1}{l_i}\Pi_{q_i}(\frac{1}{m_{Q_i}} T_{Q_i}\boldsymbol{r}_{Q_i} - M_q^{-1}\sum_j \alpha_j \boldsymbol{q}_j)$, the overall system dynamics described in (3) can be rewritten as

$$\begin{cases} \ddot{\boldsymbol{x}}_l = -\frac{1}{m_l}(T_1\boldsymbol{q}_1 + T_2\boldsymbol{q}_2) + g\boldsymbol{e}_3 \\ \ddot{\boldsymbol{q}}_i = -\|\dot{\boldsymbol{q}}_i\|^2 + \Pi_{q_i}\boldsymbol{\tau}_i \end{cases} \tag{6}$$

which highlights the similarity with the free flying quadrotor system described by

$$\begin{cases} \ddot{\boldsymbol{x}} = -\frac{T}{m}\boldsymbol{r} + g\boldsymbol{e}_3 \\ \ddot{\boldsymbol{r}} = -\|\dot{\boldsymbol{r}}\|^2 + \Pi_r, \boldsymbol{\tau} \end{cases} \tag{7}$$

much in the same way as for (7) with inputs given by $(T, \boldsymbol{\tau})$. To this end, the following assumption needs to be satisfied, to guarantee that all variables and respective time-derivatives used to define the control laws are well-defined.

Assumption 3. The desired trajectories $\boldsymbol{x}_{ld}$ are class C^5, bounded functions of time.

To further detail this strategy, consider the tracking errors $\tilde{\boldsymbol{x}}_l = \boldsymbol{x}_{ld} - \boldsymbol{x}_l$ and $\tilde{\boldsymbol{v}}_l = \dot{\boldsymbol{x}}_{ld} - \boldsymbol{v}_l$ and the PD-like controller $\boldsymbol{a}_{ld} = g\boldsymbol{e}_3 - \ddot{\boldsymbol{x}}_{ld} - k_x\tilde{\boldsymbol{x}}_l - k_v\tilde{\boldsymbol{v}}_l$. Then, the desired tensions T_{1d} and T_{2d} and desired tension directions $\boldsymbol{q}_{1d}$ and $\boldsymbol{q}_{2d}$ can be computed via (4) and (5) with $T_t\boldsymbol{q}_t = m_l\boldsymbol{a}_{ld}$. Defining

$$T_i^* = \boldsymbol{q}_i^T T_{id}\boldsymbol{q}_{id}, \tag{8}$$

the closed-loop linear dynamics can be written as

$$\begin{cases} \dot{\tilde{\boldsymbol{x}}}_l = \tilde{\boldsymbol{v}}_l \\ \dot{\tilde{\boldsymbol{v}}}_l = -k_x\tilde{\boldsymbol{x}}_l - k_v\tilde{\boldsymbol{v}}_l + \frac{T_{1d}}{m_l}\Pi_{q_1}\tilde{\boldsymbol{q}}_1 + \frac{T_{2d}}{m_l}\Pi_{q_2}\tilde{\boldsymbol{q}}_2 \end{cases} \tag{9}$$

where $\tilde{\boldsymbol{q}}_i = \boldsymbol{q}_i - \boldsymbol{q}_{id}$ gives the error between current and desired orientations. The mismatch between $\boldsymbol{q}_i$ and $\boldsymbol{q}_{id}$ can then be driven to zero by again defining PD controllers for the inputs τ_i^*, taking into account the fact that now the state $\boldsymbol{q}_i$ evolves on the two-sphere $\mathbb{S}(2)$. Rewriting the cable attitude vector error $\dot{\tilde{\boldsymbol{q}}}_i$ as

$$\begin{aligned} \dot{\tilde{\boldsymbol{q}}}_i = \dot{\boldsymbol{q}}_{id} - \dot{\boldsymbol{q}}_i = \Pi_{\boldsymbol{q}_{id}}\dot{\boldsymbol{q}}_{id} - \dot{\boldsymbol{q}}_i = -S^2(\boldsymbol{q}_{id})\dot{\boldsymbol{q}}_{id} - \dot{\boldsymbol{q}}_i \\ = S(-\tilde{\boldsymbol{q}}_i - \boldsymbol{q}_i)S(\boldsymbol{q}_{id})\dot{\boldsymbol{q}}_{id} - \dot{\boldsymbol{q}}_i \end{aligned} \tag{10}$$

and defining the angular velocity errors as $\tilde{\boldsymbol{\omega}}_i = -\dot{\boldsymbol{q}}_i - S(\boldsymbol{q}_i)S(\boldsymbol{q}_{id})\dot{\boldsymbol{q}}_{id}$ and using

$$\begin{aligned} \boldsymbol{\tau}_i^* = \Pi_{q_i}(k_q\tilde{\boldsymbol{q}}_i + k_\omega\tilde{\boldsymbol{\omega}}_i) - S(\boldsymbol{q}_i)(S(\boldsymbol{q}_{id})\ddot{\boldsymbol{q}}_{id} \\ -\dot{\boldsymbol{q}}_i\boldsymbol{q}_i^T S(\boldsymbol{q}_{id})\dot{\boldsymbol{q}}_{id}) \end{aligned} \tag{11}$$

the closed-loop dynamics for the system with state $(\tilde{\boldsymbol{q}}_i, \tilde{\boldsymbol{\omega}}_i)$ can be written as

$$\begin{cases} \dot{\tilde{\boldsymbol{q}}}_i = -S(\tilde{\boldsymbol{q}}_i)S(\boldsymbol{q}_{id})\dot{\boldsymbol{q}}_{id} + \tilde{\boldsymbol{\omega}}_i \\ \dot{\tilde{\boldsymbol{\omega}}}_i = -\ddot{\boldsymbol{q}}_i - (\Pi_{q_i} + \boldsymbol{q}_i\boldsymbol{q}_i^T)S(\dot{\boldsymbol{q}}_i)S(\boldsymbol{q}_{id})\dot{\boldsymbol{q}}_{id} \\ \quad -S(\boldsymbol{q}_i)S(\boldsymbol{q}_{id})\ddot{\boldsymbol{q}}_{id} - \Pi_{q_i}\tau_i^* \\ \quad = \boldsymbol{q}_i(\|\dot{\boldsymbol{q}}_i\|^2 - \boldsymbol{q}_i^T S(\dot{\boldsymbol{q}}_i)S(\boldsymbol{q}_{id})\dot{\boldsymbol{q}}_{id}) \\ \quad +S(\boldsymbol{q}_i)(S(\boldsymbol{q}_i)S(\dot{\boldsymbol{q}}_i)S(\boldsymbol{q}_{id})\dot{\boldsymbol{q}}_{id} - S(\boldsymbol{q}_{id})\ddot{\boldsymbol{q}}_{id}) \\ \quad -\Pi_{q_i}\tau_i^* \\ \quad = \boldsymbol{q}_i(-\dot{\boldsymbol{q}}_i^T\tilde{\boldsymbol{\omega}}_i + \|\dot{\boldsymbol{q}}_i\|^2) - \Pi_{q_i}(k_q\tilde{\boldsymbol{q}}_i + k_\omega\tilde{\boldsymbol{\omega}}_i) \end{cases} \tag{12}$$

$(\tilde{\boldsymbol{q}}_i, \tilde{\boldsymbol{\omega}}_i)$ can then be shown to converge to zero, and consequently all tracking errors also converge to zero. The following theorem summarizes these results.

Theorem 4. *Let the thrust inputs (T_1^*, T_2^*) be given by (8) and the torque inputs $(\boldsymbol{\tau}_1^*, \boldsymbol{\tau}_2^*)$ be given by (11). Then, the origin of the closed-loop system described by (9) and (12), with state $(\tilde{\boldsymbol{x}}_l, \tilde{\boldsymbol{v}}_l, \tilde{\boldsymbol{q}}_1, \tilde{\boldsymbol{\omega}}_1, \tilde{\boldsymbol{q}}_2, \tilde{\boldsymbol{\omega}}_2)$ is uniformly asymptotically stable.*

Proof. Firstly, the origin of (12) is shown to be asymptotically stable. Considering the Lyapunov function $V_q = \frac{k_q}{2}\|\tilde{\boldsymbol{q}}_i\|^2 + \frac{1}{2}\|\tilde{\boldsymbol{\omega}}_i\|^2$ and taking the time-derivative along the trajectories of the system, we obtain $\dot{V}_q = -k_\omega\tilde{\boldsymbol{\omega}}_i^T\Pi_{q_i}\tilde{\boldsymbol{\omega}}_i \leq 0$, which implies that V_q is non-increasing, all states are bounded, and the origin of (12) is uniformly stable. By showing that all states and consequently $\dot{V}_q$ are uniformly continuous and resorting to Barbalat's Lemma, we can also conclude that $\tilde{\boldsymbol{\omega}}_i$ converges to zero and $\boldsymbol{q}_i$ converges to either $\boldsymbol{q}_{id}$ or $-\boldsymbol{q}_{id}$. Additional arguments based on linearization show that the equilibrium point $-\boldsymbol{q}_{id}$ is unstable (see [6] for details). Considering now the linear dynamics (9) together with angular dynamics (12), $i \in \{1, 2\}$, we can rewrite the system in cascaded form as

$$\begin{cases} \dot{\eta} = f(\eta, \xi, t) \\ \dot{\xi} = g(\xi, t) \end{cases} \tag{13}$$

with $\eta = [\tilde{\boldsymbol{x}}_l^T\ \tilde{\boldsymbol{v}}_l^T]^T$ and $\xi = [\tilde{\boldsymbol{q}}_1^T\ \tilde{\boldsymbol{\omega}}_1^T\ \tilde{\boldsymbol{q}}_2^T\ \tilde{\boldsymbol{\omega}}_2^T]^T$. Given that the origin of $\dot{\eta} = f(\eta, 0, t)$ is globally exponentially stable (the system becomes autonomous) and the origin of $\dot{\xi} = g(\xi, t)$ is uniformly asymptotically stable, we can immediately conclude that in some bounded region all error states converge to zero and thus the origin of the full closed-loop system is uniformly asymptotically stable. □

3.4. Mapping cable tensions to quadrotor thrust forces

The outer loop controller described in the previous section considers the virtual inputs (T_1^*, τ_1^*) and (T_2^*, τ_2^*), which need to be mapped into the quadrotor virtual inputs $T_{Q_1}^*\boldsymbol{r}_{Q_1}^*$ and $T_{Q_2}^*\boldsymbol{r}_{Q_2}^*$, respectively. Using the decomposition made in thrust optimization section (full details in the main document of the proposed work) of separating $T_{Q_i}\boldsymbol{r}_{Q_i}$ into two components - one parallel and the other perpendicular to $\boldsymbol{q}_i$:

$$T_{Q_i}\boldsymbol{r}_{Q_i} = u_i\boldsymbol{q}_i + \Pi_{\boldsymbol{q}_i}T_{Q_i}\boldsymbol{r}_{Q_i},\ \textit{where}\ u_i = \boldsymbol{q}_i^T T_{Q_i}\boldsymbol{r}_{Q_i},$$

and recalling that in (3) u_i appears in the equation for $\dot{\boldsymbol{v}}_l$, whereas $\Pi_{\boldsymbol{q}_i}$ appears in the equation for $\dot{\boldsymbol{\omega}}_i$ suggest the definition of two mappings. The first between (T_1, T_2) and (u_1, u_2) and the second between (τ_1, τ_2) and $\Pi_{\boldsymbol{q}_i}T_{Q_i}\boldsymbol{r}_{Q_i}$. Using the result $u_i = (1 + \frac{m_{Q_i}}{m_l})T_i + \frac{m_{Q_i}}{m_l}\boldsymbol{q}_i^T\boldsymbol{q}_j T_j) - m_{Q_i}l_i\|\boldsymbol{\omega}_i\|^2$, an expression for the value of u_i over time is obtained by means of this expression and knowledge of T_1^*

and T_2^*. Equation (3) is then used together with (6) to obtain the second mapping

$$\begin{cases} \Pi_{q_1} T_{Q1} \boldsymbol{r}_{Q_1} = m_1 l_1 S(\boldsymbol{q}_1)\tau_1 + m_1 \Pi_{\boldsymbol{q}_1} T_2 \boldsymbol{q}_2 \\ \Pi_{q_1} T_{Q1} \boldsymbol{r}_{Q_2} = m_1 l_2 S(\boldsymbol{q}_2)\tau_2 + m_1 \Pi_{\boldsymbol{q}_2} T_1 \boldsymbol{q}_1, \end{cases}$$

and thus select each quadrotor thrust through a injective mapping

$$T_{Q_i} \boldsymbol{r}_{Q_i} = u_i \boldsymbol{q}_i + \Pi_{\boldsymbol{q_i}} T_{Q_i} \tag{14}$$

3.5. Inner loop control

In the previous section, the outer loop control scheme was fully developed. However, the assumption of the orientation dynamics being negligible, when in comparison to the position of the load and attitude control of the cables, was made. In this section, this assumption is lifted, and the inner loop control scheme developed. This is accomplished via a backstepping procedure [2]. This is accomplished by first determining the desired quadrotors thrusts $(T_{Q_i}^*, \boldsymbol{r}_{Q_i}^*)$ as functions of the virtual tensions and torques $(T_i^*, \boldsymbol{\tau}_i^*)$ and then designing a inner-loop orientation controller to take $\boldsymbol{r}_{Q_i}$ to $\boldsymbol{r}_{Q_i}^*$, which explores once again the cascaded form of the system.

By introducing the orientation equations for the thrust direction $\boldsymbol{r}_{Q_i}$

$$\begin{cases} \dot{\boldsymbol{q}}_i = -S({}^I\boldsymbol{\omega}_i)\boldsymbol{q}_i \\ \dot{R}_{Q_i} = -S(\boldsymbol{\omega}_{Q_i})R_{Q_i} \quad , \end{cases} \tag{15}$$

where $\boldsymbol{\omega}_{Q_i}$ is the angular velocity of quadrotor i, a separation between the thrust computed in the outer loop, the desired thrust $T_{Q_i}^* \boldsymbol{r}_{Q_i}^*$ and the current thrust vector $T_{Q_i}\boldsymbol{r}_{Q_i}$ is made. According to (14), the desired quadrotor thrust vectors take the form

$$\begin{aligned} T_{Q_1}^* \boldsymbol{r}_{Q_1}^* &= \boldsymbol{q}_1 (m_{Q_1} l_1 \boldsymbol{\omega}_1^T \boldsymbol{\omega}_1 + \frac{m_{Q_1} + m_1}{m_l} T_1^* \\ &+ \frac{m_{Q_1}}{m_l} \boldsymbol{q}_1^T T_2^* \boldsymbol{q}_2) + \Pi_{q_1}(m_1 l_1 \tau_1^* + m_1 T_2^* \boldsymbol{q}_2) \end{aligned} \tag{16a}$$

$$\begin{aligned} T_{Q_1}^* \boldsymbol{r}_{Q_2}^* &= \boldsymbol{q}_2 (m_{Q_2} l_2 \boldsymbol{\omega}_2^T \boldsymbol{\omega}_2 + \frac{m_{Q_2} + m_1}{m_l} T_2^* \\ &+ \frac{m_{Q_2}}{m_l} \boldsymbol{q}_2^T T_1^* \boldsymbol{q}_1) + \Pi_{q_2}(m_1 l_1 \tau_2^* - m_1 T_1^* \boldsymbol{q}_1) \end{aligned} \tag{16b}$$

Note that (16a) and (16b) are defined as functions of the real values of $\boldsymbol{q}_1$ and $\boldsymbol{q}_2$, not the desired ones. Adding and subtracting the desired thrust vector in the model equations, the overall system dynamics can be rewritten as

$$\begin{cases} \dot{\boldsymbol{v}}_l = g\boldsymbol{e}_3 \\ \qquad - \sum_i \left(\frac{T_i^*}{m_l} \boldsymbol{q}_i + M_q^{-1} \boldsymbol{q}_i \boldsymbol{q}_i^T (T_{Q_i} \boldsymbol{r}_{Q_i} - T_{Q_i}^* \boldsymbol{r}_{Q_i}^*) \right) \\ \ddot{\boldsymbol{q}}_i = -\|\dot{\boldsymbol{q}}_i\|^2 \boldsymbol{q}_i + \Pi_{q_i} \boldsymbol{\tau}_i^* \\ \qquad - \frac{1}{l_i} \Pi_{q_i} M_q^{-1} \sum_j \boldsymbol{q_j} \boldsymbol{q_j}^T (T_{Q_j} \boldsymbol{r}_{Q_j} - T_{Q_j}^* \boldsymbol{r}_{Q_j}^*) \\ \qquad + \frac{1}{m_{Q_i} l_i} \Pi_{q_i} (T_{Q_i} \boldsymbol{r}_{Q_i} - T_{Q_i}^* \boldsymbol{r}_{Q_i}^*) \end{cases}$$

Finally, setting

$$T_{Q_i} = T_{Q_i}^* \boldsymbol{r}_{Q_i}^T \boldsymbol{r}_{Q_i}^*, \tag{17}$$

where the following property was used: $\boldsymbol{v}^T \dot{\boldsymbol{v}} = 0$ for any vector $\boldsymbol{v} \in \mathbb{S}(2)$. introducing the new error variable $\tilde{\boldsymbol{r}}_{Q_i} = \boldsymbol{r}_{Q_i}^* - \boldsymbol{r}_{Q_i}$, and transforming into the error system, the full error system can be described by

$$\begin{cases} \dot{\tilde{\boldsymbol{x}}}_l = \tilde{\boldsymbol{v}}_l \\ \dot{\tilde{\boldsymbol{v}}}_l = -k_x \tilde{\boldsymbol{x}}_l - k_v \tilde{\boldsymbol{v}}_l + \frac{T_{1d}}{m_l} \Pi_{q_1} \tilde{\boldsymbol{q}}_1 + \frac{T_{2d}}{m_l} \Pi_{q_2} \tilde{\boldsymbol{q}}_2 \\ \qquad - M_q^{-1} \sum_i \boldsymbol{q}_i \boldsymbol{q}_i^T \Pi_{\boldsymbol{r}_{Q_i}} T_{Q_i}^* \tilde{\boldsymbol{r}}_{Q_i} \end{cases} \tag{18}$$

and

$$\begin{cases} \dot{\tilde{\boldsymbol{q}}}_i = -S(\tilde{\boldsymbol{q}}_i) S(\boldsymbol{q}_{id}) \dot{\boldsymbol{q}}_{id} + \tilde{\boldsymbol{\omega}}_i \\ \dot{\tilde{\boldsymbol{\omega}}}_i = \boldsymbol{q}_i (-\dot{\boldsymbol{q}}_i^T \tilde{\boldsymbol{\omega}}_i + \|\dot{\boldsymbol{q}}_i\|^2) - \Pi_{q_i}(k_q \tilde{\boldsymbol{q}}_i + k_\omega \tilde{\boldsymbol{\omega}}_i) \\ \qquad + \frac{1}{l_i} \Pi_{q_i} (M_q^{-1} \sum_j \boldsymbol{q}_j \boldsymbol{q}_j^T \Pi_{\boldsymbol{r}_{Q_j}} T_{Q_j}^* \tilde{\boldsymbol{r}}_{Q_j} \\ \qquad + \frac{1}{m_{Q_i}} \Pi_{\boldsymbol{r}_{Q_i}} T_{Q_i}^* \tilde{\boldsymbol{r}}_{Q_i}) \\ \dot{\tilde{\boldsymbol{r}}}_{Q_i} = -S(\tilde{\boldsymbol{r}}_{Q_i}) S(\boldsymbol{r}_{Q_i}^*) \dot{\boldsymbol{r}}_{Q_i}^* - \dot{\boldsymbol{r}}_{Q_i} \\ \qquad - S(\boldsymbol{r}_{Q_i}) S(\boldsymbol{r}_{Q_i}^*) \dot{\boldsymbol{r}}_{Q_i}^* \end{cases} \tag{19}$$

Again, the system takes a cascaded form and the convergence of $\tilde{\boldsymbol{r}}_{Q_i}$ to zero guarantees that there exists a neighborhood of the origin inside which all error states converge to zero. An immediate comparison can be made from the multiple quadrotor case and the single quadrotor case: the same terms are present - the terms regarding velocity error and angular velocity error, the remaining terms of the negative semi-definite function addition and the control input $\bar{\boldsymbol{\omega}}_{Q_i}$. In this case, there are additional terms due to the fact that there are two quadrotors.

Theorem 5. *Let the quadrotor thrust inputs (T_{Q_1}, T_{Q_2}) be given by (17) and the angular rate inputs $(\dot{\boldsymbol{r}}_{Q_1}, \dot{\boldsymbol{r}}_{Q_2})$ be given by*

$$\begin{cases} \dot{\boldsymbol{r}}_{Q_i} = +k_Q \Pi_{\boldsymbol{r}_{Q_i}} \tilde{\boldsymbol{r}}_{Q_i} + (\frac{T_{Q_i}^*}{m_{Q_i} l_i} \Pi_{\boldsymbol{r}_{Q_i}} \\ + \frac{T_{Q_j}^*}{l_i} (M_q^{-1} \sum_j \boldsymbol{q}_j \boldsymbol{q}_j^T \Pi_{\boldsymbol{r}_{Q_j}})) \tilde{\boldsymbol{\omega}}_i + S(\boldsymbol{r}_{Q_i}) S(\boldsymbol{r}_{Q_i}^*) \dot{\boldsymbol{r}}_{Q_i}^* \end{cases}$$

Then, the origin of the closed-loop system described by (18) and (19), with state $(\tilde{\boldsymbol{x}}_l, \tilde{\boldsymbol{v}}_l, \tilde{\boldsymbol{q}}_1, \tilde{\boldsymbol{\omega}}_1, \tilde{\boldsymbol{q}}_2, \tilde{\boldsymbol{\omega}}_2, \tilde{\boldsymbol{r}}_{Q_1}, \tilde{\boldsymbol{r}}_{Q_2})$ is uniformly asymptotically stable.

Proof. Considering the system described by (19), the Lyapunov function

$$W_i = \sum_i \left(\frac{k_q}{2} \|\tilde{\boldsymbol{q}}_i\|^2 + \frac{1}{2} \|\tilde{\boldsymbol{\omega}}_i\|^2 + \frac{1}{2} \|\tilde{\boldsymbol{r}}_i\|^2 \right) \tag{20}$$

has negative semi-definite time derivative given by

$$\dot{W}_i = -k_\omega \|\tilde{\boldsymbol{\omega}}_i\|^2 - k_Q \tilde{\boldsymbol{r}}_{Q_i}^T \Pi_{\boldsymbol{r}_{Q_i}} \tilde{\boldsymbol{r}}_{Q_i}. \tag{21}$$

Invoking once again Barbalat's Lemma, we can show that the origin of (19) is uniformly asymptotically stable. Finally, using the same cascaded form as in (13), but now with $\eta = [\tilde{\boldsymbol{x}}_l^T \ \tilde{\boldsymbol{v}}_l^T]^T$ and $\xi = [\tilde{\boldsymbol{q}}_1^T \ \tilde{\boldsymbol{\omega}}_1^T \ \tilde{\boldsymbol{q}}_2^T \ \tilde{\boldsymbol{\omega}}_2^T \ \tilde{\boldsymbol{r}}_{Q_1}^T \ \tilde{\boldsymbol{r}}_{Q_2}^T]^T$, we can again conclude that the origin of the full closed-loop system with state (η, ξ) is uniformly asymptotically stable. □

One could from equation (20), obtain the required input $\boldsymbol{\omega}_Q$, from equation (3) $\Pi_{e_3}\boldsymbol{\omega}_Q = -S(\boldsymbol{r}_{Q_i})\dot{\boldsymbol{r}}_{Q_i}$. This strategy ultimately involves less intensive computation as per using the backstepped approach for the case of one quadrotor, as the cross terms in the Lyapunov derivatives become harder to compute for each added inner loop (adding the torque equation would further complicate the computations). The added cross terms of $\tilde{\boldsymbol{q}}_i$ in the load equation cannot be crossed out directly so one would need to find suitable gains for the Lyapunov function to maintain its negative semi-definiteness.

4. Results

In this section, the simulation results are presented for a circular trajectory with fixed altitude. One term in the control law requires special attention: the time derivative of the desired orientation vector $\dot{\boldsymbol{r}}^*_{Q_i}$. This term will be computed numerically via the approximation with a band pass filter, which accurately represents this derivative for most trajectories. Considerable differences only occur when considering the first time step where there can be a step input to the derivative and trajectories with fast changing orientations, since the approximation via a low-pass filter presents some lag in the output, when compared to the analytic calculation. As presented next, this approximation does not present poor results, for the selected gains k_{Q_1} and k_{Q_2}. The alternative is to compute analytically this term, which further increases the complexity of the control scheme.

Three controllers were tested for the previous trajectories: the nonlinear Lyapunov based controller with no inner loop dynamics (assumed instantaneous), the nonlinear Lyapunov based controller with the inner loop controller proposed in this paper, and a free flying controller applied to both quadrotors. The free flying case was constructed with no information regarding disturbances and the internal forces acting on the quadrotors due to the cable connections, only adding a constant term equal to the weight of the load. The initial condition is set at $\boldsymbol{x}_l(0) = [3, 0.9375-2, A+2]^T$ m, where $A = 2$ m. This was selected in this manner as to defined an offset of $[3, -2, 2]$ m over the initial position condition that guaranteed a null position error in the circular motion trajectories. The flat output angles β_1, β_2 and γ will be kept constant at $\frac{\pi}{4}$, $\frac{\pi}{4}$, and 0 rad, respectively. The selected trajectory is given by

$$\boldsymbol{x}_{ld}(t) = \begin{bmatrix} A\sin(\omega t) \\ A\cos(\omega t) \\ 0 \end{bmatrix},$$

where $\omega = \frac{\pi}{2}$ rad/s.

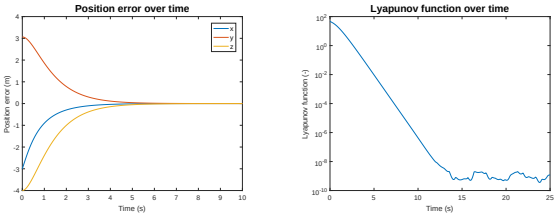

(a) Position Error (b) Lyapunov function

Figure 3: Simulation results for nonlinear model - circular trajectory with fixed altitude - no inner loop dynamics

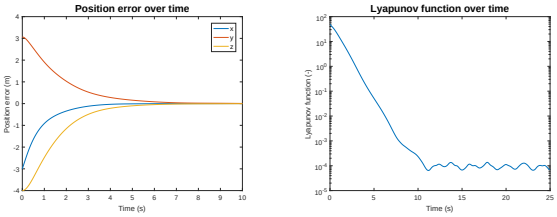

(a) Position Error (b) Lyapunov function

Figure 4: Simulation results for nonlinear model - circular trajectory with fixed altitude - full dynamics

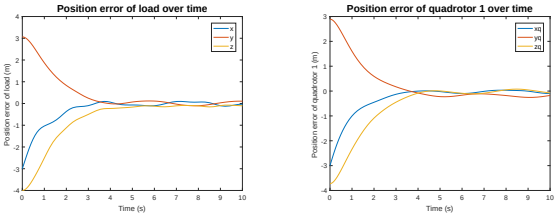

(a) Position error of load - free flying model solution (b) Position error of quadrotor 1 - free flying model solution

Figure 5: Simulation results for nonlinear model - circular trajectory with sinusoidal varying altitude - free flying

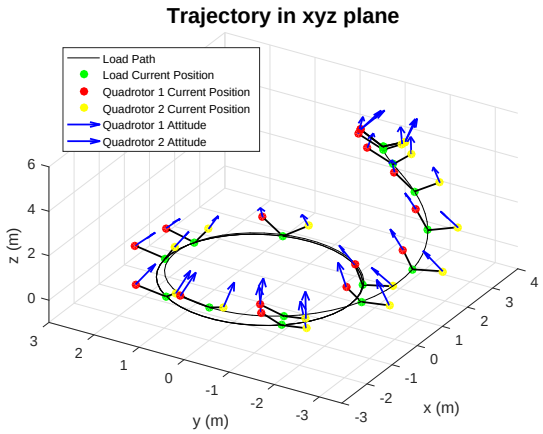

Figure 6: Trajectory in 3D - circular trajectory with fixed altitude

In Fig. 3, we can observe that the position error converges in approximately 10 seconds and the Lyapunov function reaches the value of 10^{-9} in 12 seconds, for the case where the inner loop dynamics are neglected. With the inner loop controller, as observed in Fig. 4, the position error also converges to zero. However, the mean value reached by the Lyapunov function is about 10^{-4} instead of 10^{-9}. This is likely due to the derivative term approximation, as the angular velocity error states exhibit a sinusoidal-like variation due to the added delay in the derivative term due to using a linear approximation for the time derivative. However the position error values still remain in low values, with a position error of about 0.0035 m.The 3-D trajectories of the load and quadrotors over time are shown in Fig. 6, where it is noticeable that the relative configuration of the cables remain approximately constant over time, as specified in the flat outputs. The position errors for the load and for one quadrotor are shown in Fig. 5. It can be observed that the free flying control solution does not adequately control the quadrotors to obtain the desired position, as the force interactions between the quadrotors and the load act as time-varying disturbances on the system. Neglecting these interactions causes an undamped solution, as observed in Fig. 5 b), which propagates to the position error of the load, as shown in Fig. 5 a). The z component of the quadrotor error oscillates around zero, due to the weight term added for compensation. The mean error of the load for this solution is 0.1383 m - more than 4 times the mean value for the full model solution. These oscillations can also cause practical problems with the cable's ridigity assumptions not holding valid in an experiment, compromising the quadrotor and the load.

5. Conclusions

5.1. Achievements

In this work, a novel control approach for trajectory tracking of a slung load using two quadrotors was proposed. The approach relies on the definition of a new set of flat outputs, which completely determine the relative configurations between the load and the quadrotors and have a simpler geometric interpretation than previously proposed outputs. For control system design an error system in cascaded form is incrementally constructed together with a cooperative control law for the two quadrotors that renders the origin of closed-loop system uniformly asymptotically stable. As demonstrated in the simulations in Section 4, the overall error state converges to zero, while maintaining the inputs within the physical limits of the actuators for each quadrotor.

5.2. Future Work

Future work for the problem of load transportation can be divided into several topics: generalizing the problem formulation for more than 2 quadrotors with the same notion of flat outputs; work on estimation problems in order to use this controller in practical applications; lift some cable assumptions on the model definition - namely the cables needing to be taut at all times and being massless and rigid. Preliminary work has already been done on this front. For each aspect these concepts further will be developed further.

5.3. Generalizing the problem formulation for n quadrotors

For n > 2, the problem of assigning tensions for every cable, based on a desired total tension for the load obtained through the PD control cannot be done in the same manner of selecting a desired relative angle for each cable and defining the plane the cables make, since now there exists 3 or more cables. However, one must remember there are 4n inputs on this problem. With this fact in mind, a similar approach can be used to select the cable directions. The objective here is selecting the relative angle between the cable and the desired total tension, i.e, selecting $\beta_i \in \{1,2,...,n\}$. Afterwards by selecting an azimuth angle a, relative to the auxiliary coordinate y', for every cable attitude to define it in $\mathbb{R}^3$, we are left with 3+n+2n = 3+3n flat outputs (3 for the load position, n for the yaw angle of the quadrotors and 2n for the relative angles β and a). From here, a similar expression to (4) is used:

$$\begin{aligned} \boldsymbol{q}_n = cos(\beta_n)R_{aux}\boldsymbol{e}_1 + sin(\beta_n)cos(a_n)R_{aux}\boldsymbol{e}_2 \\ +sin(\beta_n)sin(a_n)R_{aux}\boldsymbol{e}_3 = cos(\beta_n)\boldsymbol{x'} \\ +sin(\beta_n)cos(a_n)\boldsymbol{y'} + sin(\beta_n)cos(a_n)\boldsymbol{z'}, \end{aligned} \tag{22}$$

highlighting the 3D nature of this formulation. . As for the case of two quadrotors, the auxiliary rotation matrix R_{aux} depends solely on the azimuth and the elevation angle of the total thrust tension, as the new azimuth angles serves the purpose of γ on the n = 2 problem. For n = 3, these variables completely determine the cable tensions and suffice to define an output vector with the same number of variables as the input.. Solving the underlying problem is a linear problem, with some restrictions for the relative angles, to obtain a unique solution for the thrust modules For n > 3 4n-3-3n = n-3 outputs are left to choose. By selecting n-3 thrust modules for the cables' tensions, a problem that has a unique solution and defines completely the states and inputs of the full system is reached, as for the n = 2 case. For the higher order derivatives necessary for this problem, one needs to solve the same equations as those in section 3.2, for the azimuth and elevation angles' time derivatives. In the same manner, careful consideration is required to select the areas for which the derivatives are not well defined. By once again selecting them on the $x0y$ plane, only a very narrow set of implausible trajectories is discarded.

5.4. Estimation problem for cable attitude and angular velocity

Although the proposed work only focuses on the control problem for this system, in most scenarios one needs to ensure the state variables can either be directly measured or obtained by an estimator, in order to use them for feedback. To adequately test the control system separately, laboratory experiments are conducted in which motion capture systems are available to accurately measure position and velocity of the vehicles and loads and allowing to compute cable orientations over time and swing velocities. However, in outdoor environments these estimation problems pose difficulties, particularly in computing the cables' orientation over time, without the use of multiple sensors. Although there is some research on estimating the load's state in slung-load transportation, more work can be developed in this front. The work in [5] proposes a method of computing the swing-angle of the cable in the quadrotor+slung-load transportation problem, with only the use of an IMU (Inertial Measurement Unit) and a load cell. In [13], a zonotopic state estimator is used to estimate the load position and orientation in an outdoor environment.

5.5. Lifting simplifying assumptions to increase model accuracy

There are two main assumptions on the cables: they are massless and rigid. Based on these assumptions, there is work already developed in constructing flat outputs and designing trajectories, as referenced in section 3.2. However, for the case of flexible links, the use of nonlinear control approaches is very much unexplored.

The work in [4] proves differential flatness for a model that models the cables as rigid links with a point mass at the tip of every link. Consequently, one can adapt the choice of flat outputs for the angles defined previously to define a more intuitive approach to designing trajectories, while maintaining the differential flatness property.

Another approach in increasing the accuracy of the model, is to model the system again with rigid, massless links, but allowing for periods of time when the cables are not taut through the definition of a hybrid system and transitions between the different models. In [15] and [16], differential flatness is proven for the models considering the cables being taut at all times, as mentioned in section 3.2, and the hybrid system of cables becoming loose and taut, by modelling the transitions in a sequential manner. A similar adaptation to a hybrid framework as proposed in [3] and [4] can be attempted considering the set of flat outputs proposed in this thesis.

5.6. Modelling the load as a rigid body

One assumption made in the model is that the load is a point mass load, which neglects the moments applied by the cables, given that the attachment point is not in the center of mass of the load. From these interactions, a vector equation for the angular momentum of the load Ω_L appears and the control solution must take this into account, or at least ensure that the oscillations although not eliminated, are damped so the load stabilizes over the course of the prescribed trajectory.

In [7] and [18], the methodology for relative configuration of the cables with a rigid body model for the load is further developed, following a similar approach to the one made in this work. However, it still uses perturbation theory for the design of the inner loop controller, which has some limitations in gains when compared to a backstepping approach and does not use the concept of differential flatness.

Acknowledgements

The author would like to thank Prof. Rita Cunha and Prof. Paulo Oliveira for their guidance throughout the development of this work and to all my friends of family for their emotional support.

This work was supported by Fundação para a Ciência e a Tecnologia (FCT) through the project LOTUS - PTDC/EEI-AUT/5048/2014.

References

[1] D. Cabecinhas, R. Cunha, and C. Silvestre. A trajectory tracking control law for a quadrotor with slung load. *Automatica*, 2018.

[2] H. K. Khalil. *Nonlinear Systems*. Prentice Hall, Michigan, second edition, 1996.

[3] P. Kotaru, G. Wu, and K. Sreenath. Dynamics and control of a quadrotor with a payload suspended through an elastic cable. In *2017 American Control Conference (ACC)*, 2017.

[4] P. Kotaru, G. Wu, and K. Sreenath. Differential-flatness and control of quadrotor(s) with a payload suspended through flexible cable(s). In *2018 Indian Control Conference (ICC)*, 2018.

[5] S. J. Lee and H. J. Kim. Autonomous swing-angle estimation for stable slung-load flight of multi-rotor uavs. In *2017 IEEE International Conference on Robotics and Automation (ICRA)*, 2017.

[6] T. Lee. Optimal hybrid controls for global exponential tracking on the two-sphere. In *2016 IEEE 55th Conference on Decision and Control (CDC)*, pages 3331–3337, Dec 2016.

[7] T. Lee. Geometric control of quadrotor uavs transporting a cable-suspended rigid body. *IEEE Transactions on Control Systems Technology*, 2018.

[8] T. Lee, K. Sreenath, and V. Kumar. Geometric control of cooperating multiple quadrotor uavs with a suspended payload. In *Proceedings of the IEEE Conference on Decision and Control*, 2013.

[9] P. Martin, P. Rouchon, and R. M. Murray. Flat Systems, Equivalence and Trajectory Generation. Technical report, Control and Dynamic Systems, California Institute of Technology, 2003.

[10] D. Mellinger and V. Kumar. Minimum snap trajectory generation and control for quadrotors. In *2011 IEEE International Conference on Robotics and Automation*, 2011.

[11] P. O. Pereira and D. V. Dimarogonas. Control framework for slung load transportation with two aerial vehicles. In *2017 IEEE 56th Annual Conference on Decision and Control (CDC)*, 2017.

[12] P. O. Pereira, M. Herzog, and D. V. Dimarogonas. Slung load transportation with a single aerial vehicle and disturbance removal. In *2016 24th Mediterranean Conference on Control and Automation (MED)*, 2016.

[13] B. S. Rego and G. V. Raffo. Suspended load path tracking control based on zonotopic state estimation using a tilt-rotor uav. In *2016 IEEE 19th International Conference on Intelligent Transportation Systems (ITSC)*, 2016.

[14] J.-J. Slotine and W. Li. *Applied Nonlinear Control*. Prentice-Hall, 1991.

[15] K. Sreenath and V. Kumar. Dynamics, Control and Planning for Cooperative Manipulation of Paylods Suspended by Cables from Multiple Quadrotor Robots. In *Robotics: Science and Systems 2013*, 2013.

[16] K. Sreenath, N. Michael, and V. Kumar. Trajectory generation and control of a quadrotor with a cable-suspended load-A differentially-flat hybrid system. In *Proceedings of the 2013 IEEE International Conference on Robotics and Automation (ICRA)*, 2013.

[17] D. K. D. Villa, A. S. Brandão, and M. Sarcinelli-Filho. Load transportation using quadrotors: A survey of experimental results. In *2018 International Conference on Unmanned Aircraft Systems (ICUAS)*, 2018.

[18] G. Wu and K. Sreenath. Geometric control of multiple quadrotors transporting a rigid-body load. In *53rd IEEE Conference on Decision and Control*, 2014.